International Journal of Mathematics and Statistics Invention (IJMSI)
E-ISSN: 2321- 4767 P-ISSN: 2321-4759
www.ijmsi.org Volume 9 Issue 3 || March, 2021 || PP 20-31

Numerical solution for boundary layer flow of a Maxwell fluid over a stretched surface with Cattaneo-Christov heat flux in the presence of heat generation and chemical reaction

M. Sreedhar Babu[1], V.Venkata Ramana[2] and P.Sireesha Devi[3]
[1,2]*Department of Applied Mathematics, Y.V. University, Kadapa, A.P.-516005, India.*
[3]*Department of Mathematics, Anurag University, Hyderabad, Telangana-500088, India*

ABSTRACT
The process pertaining to the numerical simulation of Cattaneo-Christov heat flux model for Maxwell fluid past a stretching surface in the presence of mass transfer, heat generation or absorption and first order chemical reaction has been examined here. The Numerical solutions have been computed via the 4th order Runge-Kutta method along with the shooting technique. The resulting similarity solutions have been calculated and presented graphically for the non-dimensional velocity, temperature, and concentration, local rate of heat and mass transfer with pertinent parameters. Verification of results has been made with earlier results for Maxwell fluid flow and clear fluid studies. Specific problems have several applications in the engineering and petroleum industries, like electroplating, chemical processing of heavy metals and solar water heaters.

KEYWORDS: *Maxwell fluid, hear and mass transfer, heat generation or absorption, chemical reaction*

Date of Submission: 29-03-2021 Date of Acceptance: 12-04-2021

I. INTRODUCTION

The occasion of warmth move wins thinking about the ability in temperature amid things or between diverse bits of a relative article. The all around saw warmth conveyance law, is known as 'Fourier's law', anticipated by Fourier [1] gives a perspective into the radiance move examination. Regardless, this edict grounds a metaphorical energy stipulation, which gathers that any essential irritation is quickly felt in the course of the middling underneath assessment. Considering this test, Cattaneo [2] reconsidered this law by toting up a delivering up time tenure. From that point on, Christov [3] changed the Cattaneo sculpt by dislodging the standard subordinate among Oldroyd's upper-convected assistant. This sculpt is seen as the Cattaneo-Christov heat change sculpt. Straughan [4] considered warm convection in a level stratum of an incompressible Newtonian watery by via the Cattaneo-Christov model. Ciarletta and Straughan [5] showed brand name & adequacy of answers for the Cattaneo-Christov state of affairs. By via the Cattaneo–Christov sculpt, Tibullo and Zampoli [6] examined the rareness of answers for incompressible fluids.

The Maxwell liquid mold is perhaps the most clear and best viscoelastic molds that can manage the impact of liquid relaxing up era. Taking into account these grounds, this model has gotten the solitary considered examiners. Han et al. [7] utilized the upper-convected Maxwell (UCM) mold and Cattaneo-Christov heat change sculpt to analyze the sparkle move and cutoff layer stream of viscoelastic liquid over a growing platter amid speed slip limit by utilizing the homotopy assessment strategy (HAM). Mustafa [8] likewise utilized HAM to research the turning stream of UCM liquid in the course of the Cattaneo-Christov heat progress sculpts. Khan et al. [9] broke down the cutoff stratum stream of UCM liquid incited by an essentially extending pane utilizing the Cattaneo-Christov sculpts. Hayat et al. [10] explained the effect of Cattaneo-Christov heat change in the stream ended an expanding sheet with variable thickness. Gangadhar et al. [11] inspected mathematically the gleam move in MHD Carreau liquid over growing chamber amid the Cattaneo - Christov heat progress hypothesis. Gangadhar et al. [12] utilized the apparition relaxing up procedure to isolate the nanofluid ended a growing chamber with the Cattaneo - Christov heat development hypothesis.

Streams including impacts of the substance responses have secured the prospect of the two specialists and trained professionals. Businesses of these streams in different cycles may combine the development of ceramics and polymers, substance preparing, tasteless protections, water & air debasements and atomic dissipating of sorts. Compound responses are separate as homogeneous-heterogeneous (h and h) responses. The space as a result of heterogeneous responses at any rate confined covers the whole stage dependably. Devouring and catalysis swathe together h and h responses. Also, the diverse improvement is found in the strong stage while the harmonized motivation subsists in vaporous and fluid stages. New evaluations including the effects of h and h responses join an assessment by Imran et al. [13] who analyzed the development of Casson liquid

mathematically among impacts of h and h responses amid magneto hydrodynamics and gooey disseminating. Hayat et al. [14] inspected the wise strategy of 2D little polar liquid with h and h responses and magneto hydrodynamics. The development of 3D Oldroyd-B liquid stream by nonlinear warm radiation and homogeneous-heterogeneous (h-h) responses is investigated by Lu et al. [15]. Abbas and Sheik [16] mathematically settled the arrangement of Ferrofluid by nonlinear skid stipulation and h and h responses. Nadeem et al. [17] examined the impact of charming dipole mathematically, precedent a comprehensive chamber with h and h responses. Raju et al. [18] discovered twofold blueprints of Jeffrey liquid stream mathematically with the effect of h and h responses. Imad Khan et al. [19] examined the Prandtl liquid stream with h and h responses past a direct expanded surface. Of late, impacts of substance response and convective condition on wandering distorted liquid past a solid expanded surface was engaged by Gangadhar et al. [20].

In certain fluid applications, working fluid warmth age (source) or ingestion (sink) impacts are huge. Test examines dealing with these effects have been represented by makers, for instance, Qasim [21] who broke down meanwhile the possessions of warmth and mass trade on non-Newtonian Jeffrey's viscoelastic fluid stream inside seeing warmth source/sink. Gangadhar et al. [22] explored the breaking point layer stream assessment of nanofluids over an all-inclusive surface with heat age/maintenance, variable attractions/implantation and gooey scattering impacts.

In the light of the above assessments, the objective of the current assessment is to exhibit the effect of warmth age or absorption and first solicitation manufactured reaction ramifications for laminar breaking point layer stream of a Maxwell fluid past broadened surface by Cattaneo-Christov heat progress speculation. The overseeing plan of mostly differential conditions is non-dimensionalized and changed keen on the standard differential conditions and settled numerically via using the RK fourth solicitation way. Likenesses are investigated by the open domino effects in a restraining comportment. The possessions of remembered limits for the speed, temperature and center pastures are scrutinized and discussed.

II. MATHEMATICAL FORMULATION

Imagine a laminar limit stratum two-dimensional progression of incompressible, upper-convected Maxwell liquid precedent an extending facade with heat age or ingestion and first request compound response. The warmth move measure is concentrated in the course of the Cattaneo – Christov heat motion hypothesis. The surface overlaps amid the flat $\bar{y} = 0$ and the gush curbed to $\bar{y} > 0$. The gush is spawned owing to linear broadening of the surface down to the synchronized relevancies of two like and reverse forces beside the $\bar{x}$ - axis as revealed in the Fig.1. Keeping the origin preset, the facade is then lingering among haste $u_w(\bar{x}) = a\bar{x}$ where $a > 0$ the elongating tempo and $\bar{x}$ - harmonize measured beside the stretching facade, untrustworthy linearly by a distance from the gash. The ambient fluid temperature is a constant $\overline{T}_\infty$ and the ambient fluid attentiveness is a constant $\overline{C}_\infty$.

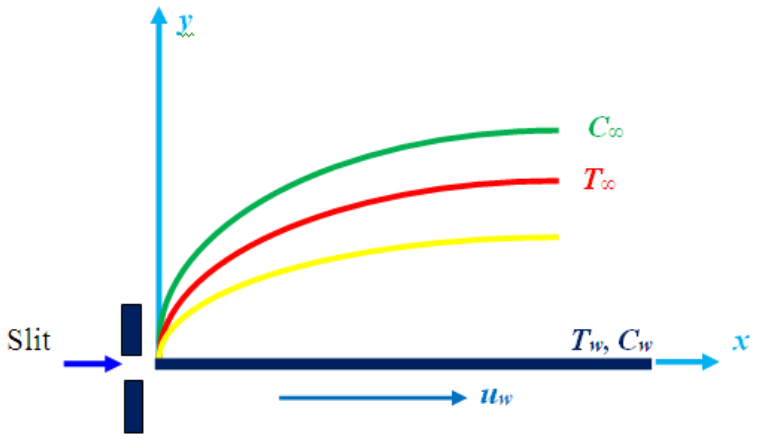

Fig. 1: Physical model and coordinate system

In the dearth of the pitch of pressure, the prevailing equations uttering upkeep of mass, momentum, energy and species are prearranged as tags on:

$$\frac{\partial \bar{u}}{\partial \bar{x}} + \frac{\partial \bar{v}}{\partial \bar{y}} = 0 \quad , \qquad (1)$$

$$\bar{u}\frac{\partial \bar{u}}{\partial \bar{x}} + \bar{v}\frac{\partial \bar{u}}{\partial \bar{y}} + \lambda_1\left(\bar{u}^2\frac{\partial^2 \bar{u}}{\partial \bar{x}^2} + \bar{v}^2\frac{\partial^2 \bar{u}}{\partial \bar{y}^2} + 2\bar{u}\bar{v}\frac{\partial^2 \bar{u}}{\partial \bar{x}\partial \bar{y}}\right) = \frac{\mu}{\rho}\frac{\partial^2 \bar{u}}{\partial \bar{y}^2}, \qquad (2)$$

$$\bar{u}\frac{\partial \bar{T}}{\partial \bar{x}} + \bar{v}\frac{\partial \bar{T}}{\partial \bar{y}}$$

$$+ \lambda_2\left(\bar{u}\frac{\partial \bar{u}}{\partial \bar{x}}\frac{\partial \bar{T}}{\partial \bar{x}} + \bar{v}\frac{\partial \bar{v}}{\partial \bar{y}}\frac{\partial \bar{T}}{\partial \bar{y}} + \bar{u}\frac{\partial \bar{v}}{\partial \bar{x}}\frac{\partial \bar{T}}{\partial \bar{y}} + \bar{v}\frac{\partial \bar{u}}{\partial \bar{y}}\frac{\partial \bar{T}}{\partial \bar{x}} + \bar{u}^2\frac{\partial^2 \bar{T}}{\partial \bar{x}^2} + \bar{v}^2\frac{\partial^2 \bar{T}}{\partial \bar{y}^2} + 2\bar{u}\bar{v}\frac{\partial^2 \bar{T}}{\partial \bar{x}\partial \bar{y}}\right) \qquad (3)$$

$$= \alpha\frac{\partial^2 \bar{T}}{\partial \bar{y}^2} + \frac{Q_0}{\rho c_p}(\bar{T} - \bar{T}_\infty),$$

$$\bar{u}\frac{\partial \bar{C}}{\partial \bar{x}} + \bar{v}\frac{\partial \bar{C}}{\partial \bar{y}} = D\frac{\partial^2 \bar{C}}{\partial \bar{y}^2} - k_0(\bar{C} - \bar{C}_\infty), \qquad (4)$$

Where $\bar{u}$ & $\bar{v}$ refer to velocity apparatus by the side of $\bar{x}$ - & $\bar{y}$ - directions, in that order. $\upsilon = \mu/\rho$ - kinematic tackiness, μ - fluid viscosity, λ_1 - fluid relaxation time, λ_2 - thermal relaxation time, $\bar{T}$ - temperature of Maxwell fluid, $Q_0\,(j\,s^{-1}m^{-3}K^{-1})$ - dimensional heat generation $Q_0 > 0$ or absorption $Q_0 < 0$ coefficient, $\bar{C}$ - Maxwell fluid concentration, ρ -fluid concreteness, c_p - fluid heat competence, k_0 - chemical reaction rate coefficient & $\alpha = k/\rho c_p$ - thermal diffusivity, where k - thermal conductivity.

The frontier conditions in the nearby quandary are

$$\bar{u} = u_w(\bar{x}) = a\bar{x},\ \bar{v} = 0,\ \bar{T} = \bar{T}_w,\ \bar{C} = \bar{C}_w, \qquad \text{at} \quad \bar{y} = 0 \qquad (5)$$

$$\bar{u} \to 0,\ \bar{T} \to \bar{T}_\infty,\ \bar{C} \to \bar{C}_\infty, \qquad \text{as} \quad \bar{y} \to \infty \qquad (6)$$

In the beyond equation, $\bar{T}_w$ - wall temperature, & $\bar{C}_w$ - wall temperature.

By using these renovations, we have

$$\xi = \sqrt{\frac{a}{\nu}}\bar{y},\ \psi = \sqrt{\nu a}\,\bar{x}\,f(\xi),\ \theta(\xi) = \frac{\bar{T} - \bar{T}_\infty}{\bar{T}_w - \bar{T}_\infty},\ \phi(\xi) = \frac{\bar{C} - \bar{C}_\infty}{\bar{C}_w - \bar{C}_\infty} \qquad (7)$$

In which ψ - stream function, equations (2) - (4) can be abridged to an organism of two tied usual differential equations as tags on:

$$f''' - f'^2 + f f'' + \beta\left(2 f f' f'' - f^2 f'''\right) - k_p f' = 0 \qquad (8)$$

$$\frac{1}{\Pr}\theta'' + f\theta' - \gamma\left(f f'\theta' + f^2\theta''\right) + Q\theta = 0 \qquad (9)$$

$$\frac{1}{Sc}\phi'' + f\phi' - Kr\,\phi = 0 \qquad (10)$$

Where prime is designates derivatives a propos ξ . The Prandtl number is prearranged as $\Pr = \upsilon/\alpha$, where α - thermal diffusivity. $\beta = \lambda_1 a$ - Deborah number & $\gamma = \lambda_2 a$ - non – dimensional thermal respite time, where a - affirmative constant, λ_1 - fluid relaxation time, λ_2 - thermal relaxation time, $Q = \frac{Q_0}{\rho a c_p}$ - heat source or sink parameter, $Kr = \frac{k_0}{a}$ - chemical retort constraint, and $Sc = \upsilon/D$ - Schmidt number. The periphery state of affairs for equations (6) and (7) are

$$f = 0,\ f' = 1,\quad \theta = 1,\quad \phi = 1, \qquad \text{at} \quad \xi = 0 \qquad (11)$$

$$f' \to 0,\quad \theta \to 0,\quad \phi \to 0, \qquad \text{as} \quad \xi \to \infty \qquad (12)$$

The corporal extents of interest are skin abrasion coefficient C_f, local Nusselt number Nu and local Sherwood number Sh, which are cleared as

$$C_f = \frac{\tau_w}{\rho u_w^2},\ Nu = \frac{\bar{x} q_w}{k(T_w - T_\infty)},\ Sh = \frac{\bar{x} q_m}{D(C_w - C_\infty)}, \tag{13}$$

Where facade trim stress τ_w, facade reheat flux q_w & facade heap flux q_m are prearranged by

$$\tau_w = \mu\left(\frac{\partial \bar{u}}{\partial \bar{y}}\right)_{\bar{y}=0},\quad q_w = -k\left(\frac{\partial \bar{T}}{\partial \bar{y}}\right)_{\bar{y}=0},\quad q_m = -D\left(\frac{\partial \bar{C}}{\partial \bar{y}}\right)_{\bar{y}=0} \tag{14}$$

With μ being lively viscosity, *k* & *D* is being thermal & mass conductivity's. Using likeness renovations (7), we obtain

$$\sqrt{\mathrm{Re}}\ C_f = f''(0),\quad \frac{Nu}{\sqrt{\mathrm{Re}}} = -\theta'(0),\quad \frac{Sh}{\sqrt{\mathrm{Re}}} = -\phi'(0), \tag{15}$$

Where $\mathrm{Re} = \frac{a\bar{x}^2}{\upsilon}$ -local Reynolds number.

2.1 SOLUTION PROCEDURES USING THE SHOOTING METHOD:

The mathematical strategy used to address the differential framework Eqs. (8) - (10). This framework alongside the limit conditions Eqns. (11) - (12) is coordinated mathematically by methods for the Runge-Kutta strategy with a methodical gauge of $f''(0), \theta'(0)$ and $\phi'(0)$ by the Newton-Raphson shooting procedure until the limit conditions at the endlessness $f'(\infty),\ \theta(\infty)$ and $\phi'(\infty)$ rot dramatically to nothing. In this strategy it is important to pick a reasonable limited worth, for which the accompanying first-request framework is set. Equations (8)-(10) amid boundary state of affairs (11) – (12) are then abridged to an organism of initial sort

$$y_1 = f,\ y_2 = f',\ y_3 = f'',\ y_4 = \theta,\ y_5 = \theta',\ y_6 = \phi,\ y_7 = \phi'$$

$$y_3' = -\frac{1}{(1 - \beta\ y_1^2)}(y_1 y_5 - y_2^2 + 2\beta\ y_1 y_2 y_3),\ y_3(0) = \varepsilon_1$$

$$y_1(0) = 0,\ y_2(0) = 1,\ y_2(\infty) = 0$$

ordinary differential equations

$$y_5' = -\frac{\mathrm{Pr}}{(1 - \gamma\ \mathrm{Pr}\ y_1^2)}(y_1 y_5 - \gamma\ y_1 y_2 y_5 + Q y_4),\ y_5(0) = \varepsilon_2$$

$$y_4(0) = 1,\ y_4(\infty) = 0$$

$$y_7' = -Sc\ y_1 y_7 + Kr\ Sc\ y_6,\ \ y_7(0) = \varepsilon_3$$

$$y_6(0) = 1,\ y_6(\infty) = 0$$

The shooting strategy is utilized to figure $\varepsilon_1, \varepsilon_2$ and ε_3 by cycles until the external limit conditions $y_2(\infty),\ y_4(\infty)$ and $y_6(\infty)$ are fulfilled. The subsequent differential conditions can be incorporated by the Runge-Kutta fourth request mixes conspire. The above methodology is rehashed until we get the outcomes up to the ideal level of exactness 10-6. The nitty gritty examination is introduced in the accompanying sections.

2.2 VALIDATION OF THE NUMERICAL PROCEDURE:

For confirmation, the upshots were dispirited & recently detailed upshots in the inscription. The aftereffects of the investigations were contrasted and the current writing for the specific inferences of torrent boundaries. These associations are publicized in Tables 1, 2 and 3. They were discovered palatable and in adequate consensus with the in progress upshots with insignificant blunders.

III. COMPUTATIONS AND DISCUSSION:

The changed force stipulation (8), energy stipulation (9) and species stipulation (10) exposed to the limit states of stipulation (11) and (12) were mathematically tackled by methods for the R-K fourth request strategy. The calculations for the RK strategy were made by utilizing MATLAB. Mathematical calculations have been introduced for different estimations of the boundaries in question, specifically β, γ, Q, Pr, Kr, and Sc that depict the stream attributes, warmth and mass exchange and the outcomes are introduced as far as visual

aids and tables. In figs 2-10 the associated in sequence: Pr = 2, $\beta = \gamma = 0.2$, Q = 0.2, Kr = 0.1, and Sc = 2.62 is by and large used (except if in any case expressed):

The flexibility number is significant for viscoelastic materials. If $\beta < 1$, it relates to the liquids, along these lines a more modest flexibility number $(\beta < 1)$ describes simply thick conduct of liquids. Actually, for $\beta > 1$, the liquid carries on like material that is flexibly strong. Because of this, the greatness of speed is bigger in more modest β liquids. By utilizing RKF, the estimation of on account of β = 1 is - 1.241748, while $\theta'(0)$ is - 0.558514, $\phi(0)$ is - 1.621043 at γ = 0.2.

Figures 2, 3 and 4 show the end product of the flexibility boundary β on the speed, temperature and focus silhouettes. The flexible power vanishes when $\beta = 0$ and the liquid turns into a Newtonian liquid. From Fig. 2, it is seen that with the expansion of β , the speed circulation shows diminishing conduct. Truly, higher β shows more grounded thick power which confines the smooth movement, and thusly the speed diminishes. The response of β on the temperature profiles are introduced for Fig. 3. Temperature profiles increment for higher estimations of β . The expanded boundary of β compares to enormous unwinding time, which gives opposition of the smooth movement, and therefore more warmth, is created. Along these lines are temperature dispersion increases. Qualities of β on the focus dissemination are portrayed in Fig. 4. It is obviously seen that the appropriations of fixation are expanded because of expanding estimations of β . The end product of non-dimensional warmth motion unwinding time γ on temperature conveyance can be clarified by Fig. 5 for both warmth age (Q>0) and warmth assimilation (Q<0). Temperature profiles are a diminishing capacity of warm unwinding boundary. It is likewise seen that the warm limit layer thickness diminishes. This is because of the way that as the warm unwinding boundary expands; specks of the fabric entail more opportunity to move warmth to their adjoining specks. All in all, non-finishing up conduct appeared by the higher estimations of warm unwinding boundary material is liable for decrease of temperature conveyance. As of this stature, it is seen that the limit layer created more warmth energy into the stream and accordingly raised the temperature profile of the stream because of expansion in heat age or ingestion boundary Q.

Figure 6 is evidences for that an augmentation in Prandtl number Pr logically diminishes temperature silhouette & thusly decreases warm limit stratum depth. The elevated Prandtl number qualities examined, i.e., Pr>1 are illustrative of polymeric non-Newtonian liquids. Prandtl nomber characterizes the proportion amid energy diffusivity and warm diffusivity. Higher estimations of Prandtl number are related among lesser warm diffusivity. Additionally, the Prandtl number is conversely corresponding to warm conductivity. Polymers have poorer warm conductivities & in this way privileged Prandtl numbers than, pro instance, fluid metals. The decline in warm conductivity with more noteworthy is Prandtl number outcomes in a solid diminishing in temperatures in the limit stratum.

Figure 7 and 8 show the reaction in fixation profile with synthetic response boundary (Kr) and Schmidt number (Sc). Figure 7 show that expanding substance response boundary (Kr) causes a stamped decrease in the focus silhouette. The response tenure in the dimensionless fixation limit stratum Eq. (14), i.e., $-Kr\phi$ depends on a first-request irrevocable synthetic response which happens both in the greater part of the liquid (synchronized) just as at the divider which is thought to be synergist to substance response. Albeit substance responses by and large can be categorized as one of two classifications, i.e., homogenous or assorted, the previous is of concern in the current examination. Homogenous compound responses happen consistently all through a given stage and apply a comparative impact to an interior wellspring of warmth age. The damaging kind of homogenous compound response was contemplated. Expanding the substance response boundary (Kr) creates a reduction in speed. The force of the limit layer thickness is along these lines increments significantly because of the impact of a more prominent compound response. It is seen that fixation circulations decline when the synthetic response increments. Actually, for a dangerous case, compound response happens and logically annihilates the first species, diffusing in the polymeric viscoelastic liquid. This, thusly, smothers atomic dissemination of the leftover species which prompts a fall in fixation extents and an abatement in the focus limit layer thickness. A figure 8 confirms to an augmentation in Schmidt number (Sc) diminishes the fixation sizes unequivocally, i.e., decreases/morals. The Schmidt number encapsulates the proportion of the energy to the throng diffusivity, i.e., Sc = υ/D. The Schmidt number in this manner evaluates the overall adequacy of energy and mass vehicle by dissemination in the hydrodynamic (speed) and fixation (genus) limit stratums. For Sc>1, energy, the dispersion rate surpasses the species dissemination pace. The inverse pertains for Sc<1. For Sc = 1, together force and fixation (sorts) limit stratums will have a similar breadth, and diffusivity tariffs will be equivalent. It is seen that

as the Schmidt number builds, the silhouettes of the fixation steadily decline. More modest estimations of Sc are identical to the increment in the compound atomic diffusivity and the other way around for bigger estimations of Sc. Fixation limit layer thickness is hence fundamentally diminished with a more prominent Schmidt number.

At last, the impact of actual amounts of interest, for example, the Nusselt number and the Sherwood number for different estimations of dimensionless administering stream field boundaries are charted in Figs 9 and 10 individually. Figure 9 shows the impacts of the Deborah number β and the warm unwinding boundary γ . It is seen that Nusselt number qualities, diminishes amid swell in though it increments because of augmentation in γ .

IV. CONCLUSION:

The limit layer brook of the Maxwell liquid past a lengthening facade is genuinely inspected contained by the sight of warmth age or assimilation under the main request compound response. The administering incomplete differential conditions were changed into an arrangement of standard differential conditions utilizing similitude change prior to being settled mathematically. The effect of versatility number β, non-dimensional warm unwinding time γ, Prandtl number Pr, heat age or ingestion boundary Q, compound response boundary Kr and Schmidt number Sc has been investigated. The fundamental discoveries can be summed up as follows:

(1) Velocity profiles diminished because of expansion in versatility boundary.

(2) An expansion in temperature profiles is a component of an increment in versatility number, heat age or assimilation boundary while warm limit layer thickness and temperature extents decline for huge estimations of non-Fourier Deborah number & Prandtl number.

(3) Attentiveness extents are smothered among huge estimations of Schmidt number & compound response boundary while it increments because of expansion in versatility boundary.

(4) The pace of warmth move diminishes because of expansion in versatility number while it increments because of expansion in warm unwinding boundary.

(5) There is an ascent in the mass exchange rate because of expansion in the synthetic response boundary while a fall is seen in the mass exchange rate because of expansion in the versatility number.

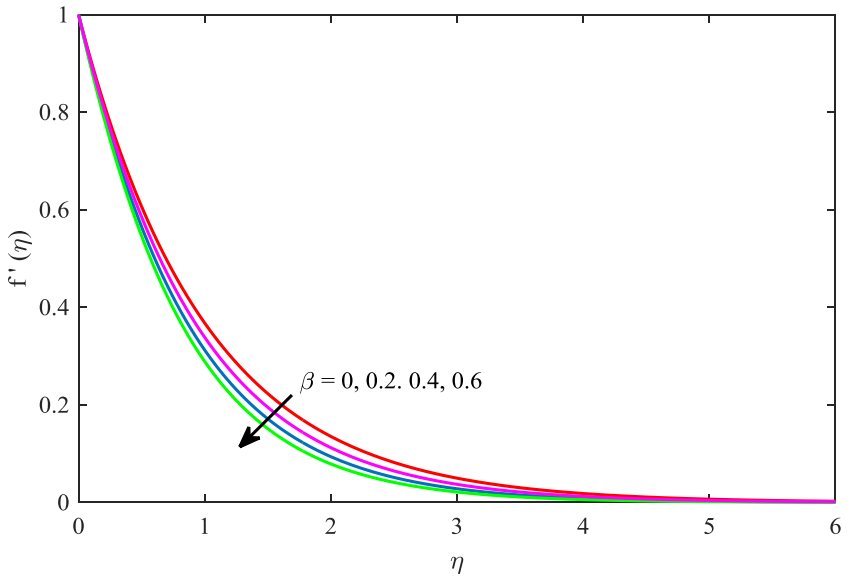

Fig. 2: Velocity distribution $f'(\eta)$ for diverse morals of β .

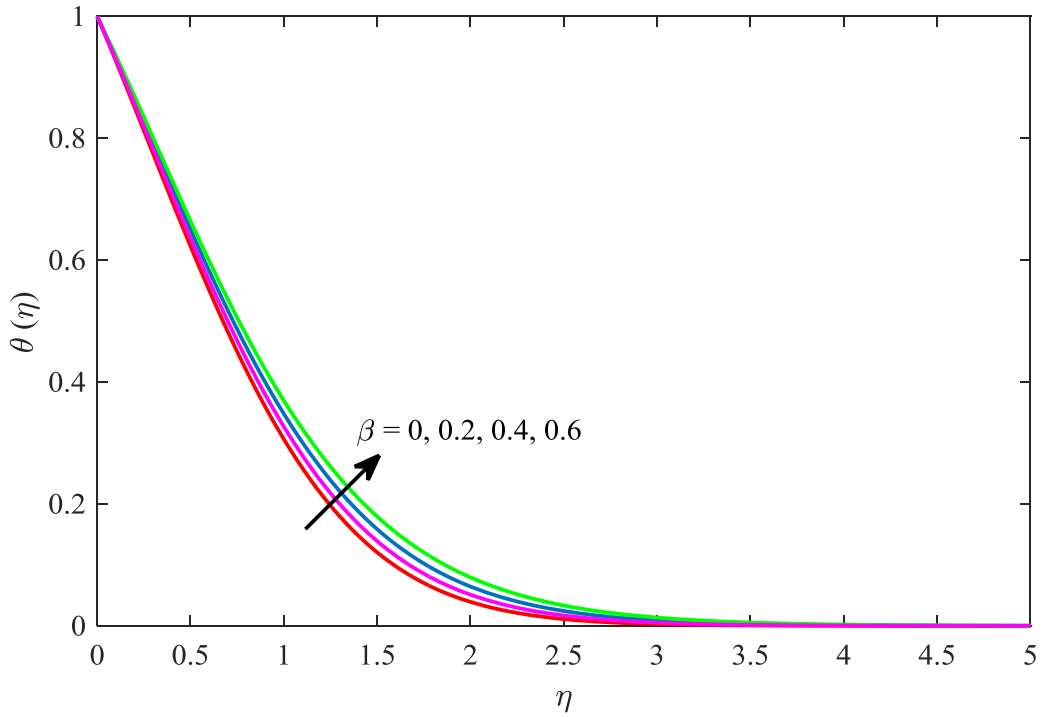

Fig. 3: Temperature distribution $\theta(\eta)$ for diverse morals of β .

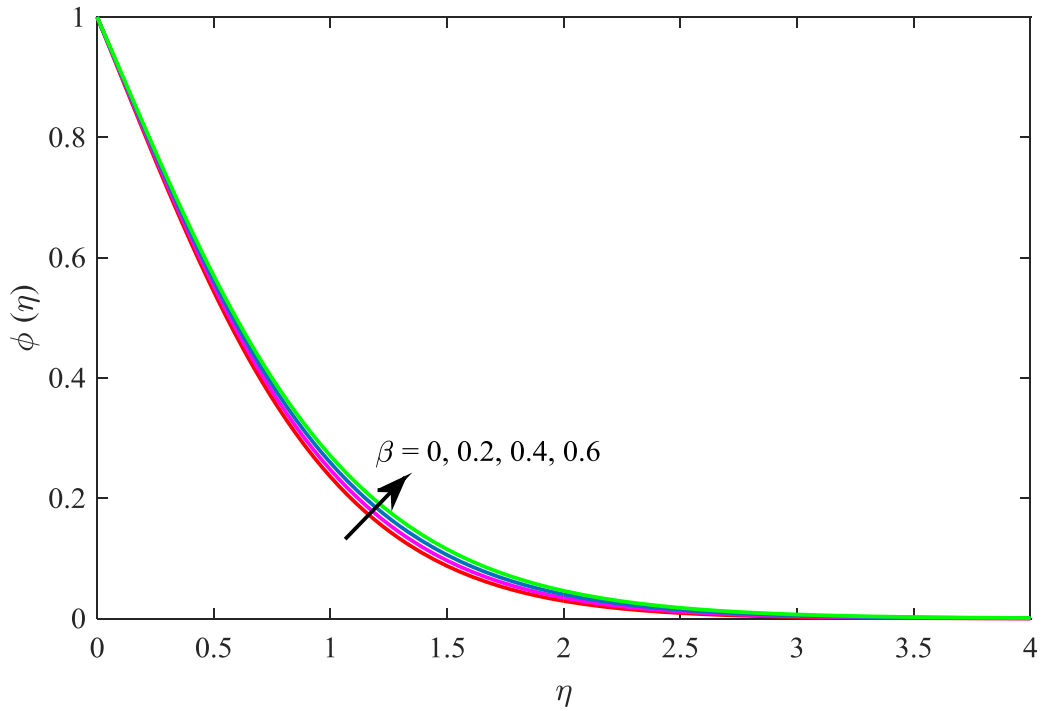

Fig. 4: Concentration distribution $\phi(\eta)$ for diverse morals of β .

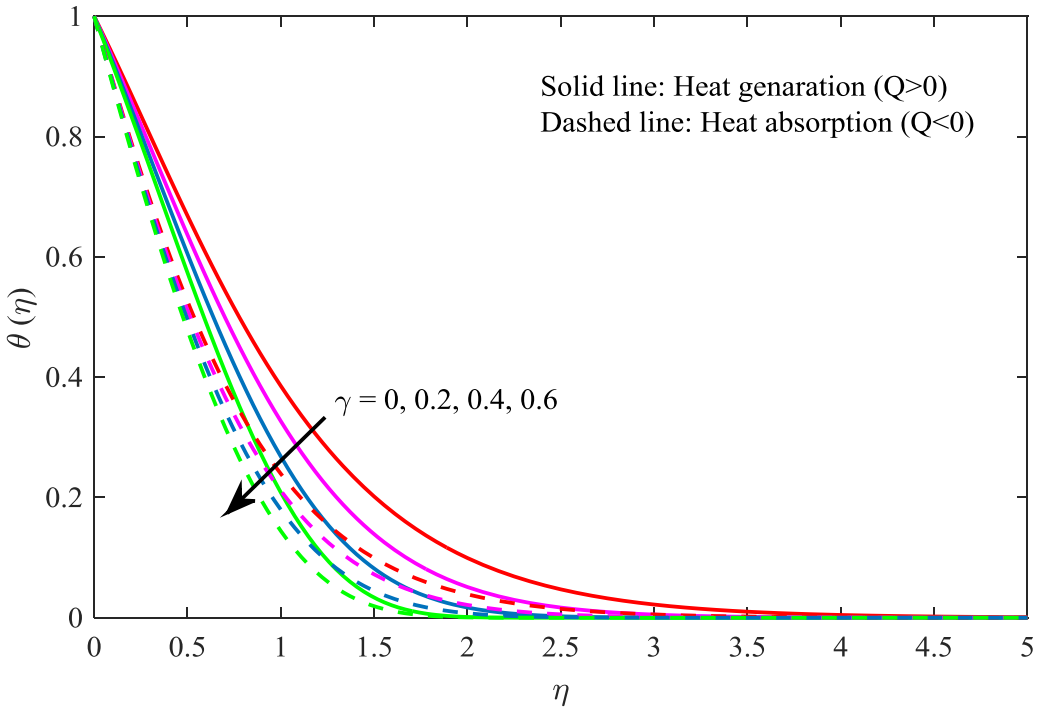

Fig. 5: Temperature distribution $\theta(\eta)$ for diverse morals of γ and Q.

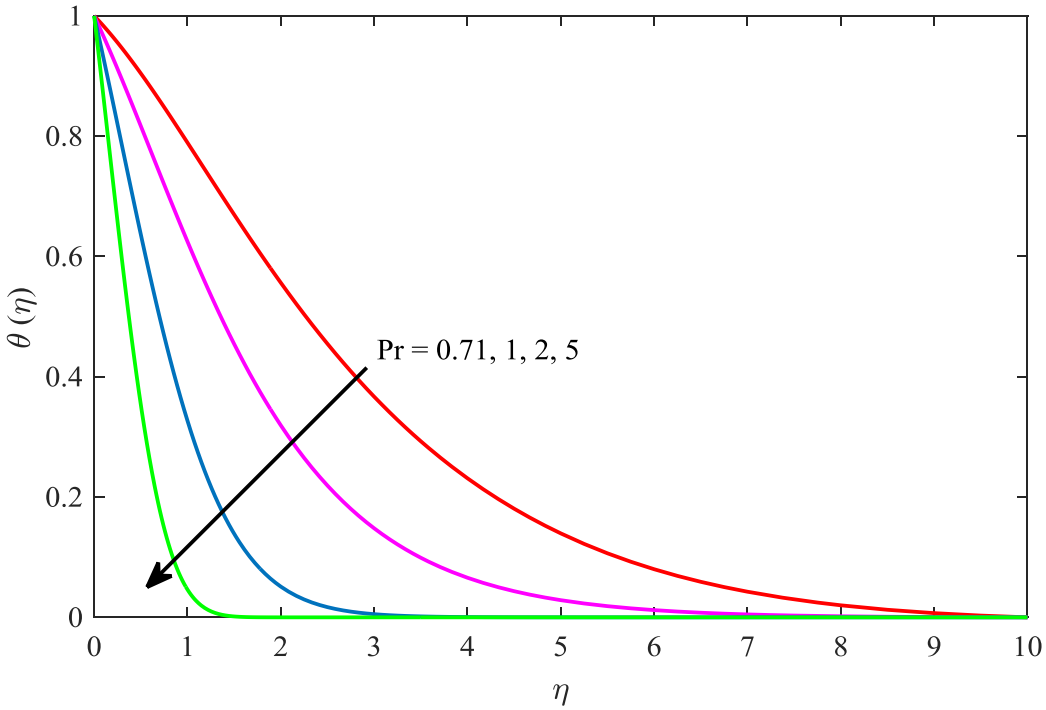

Fig. 6: Temperature distribution $\theta(\eta)$ for diverse morals of *Pr*.

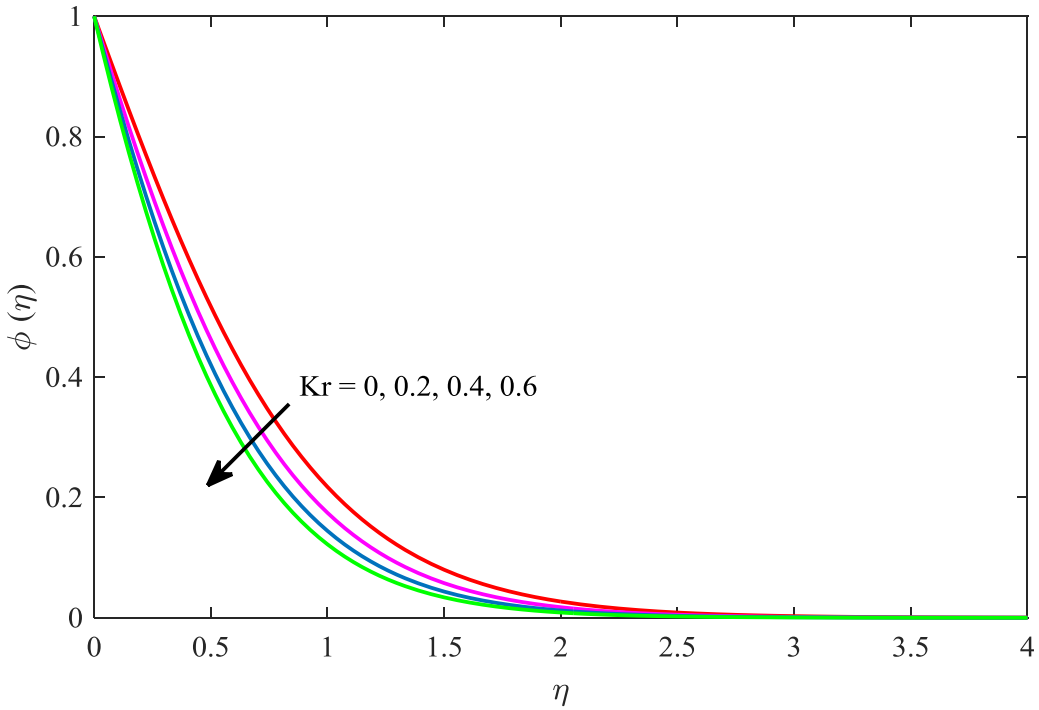

Fig. 7: Concentration distribution $\phi(\eta)$ for diverse morals of Kr .

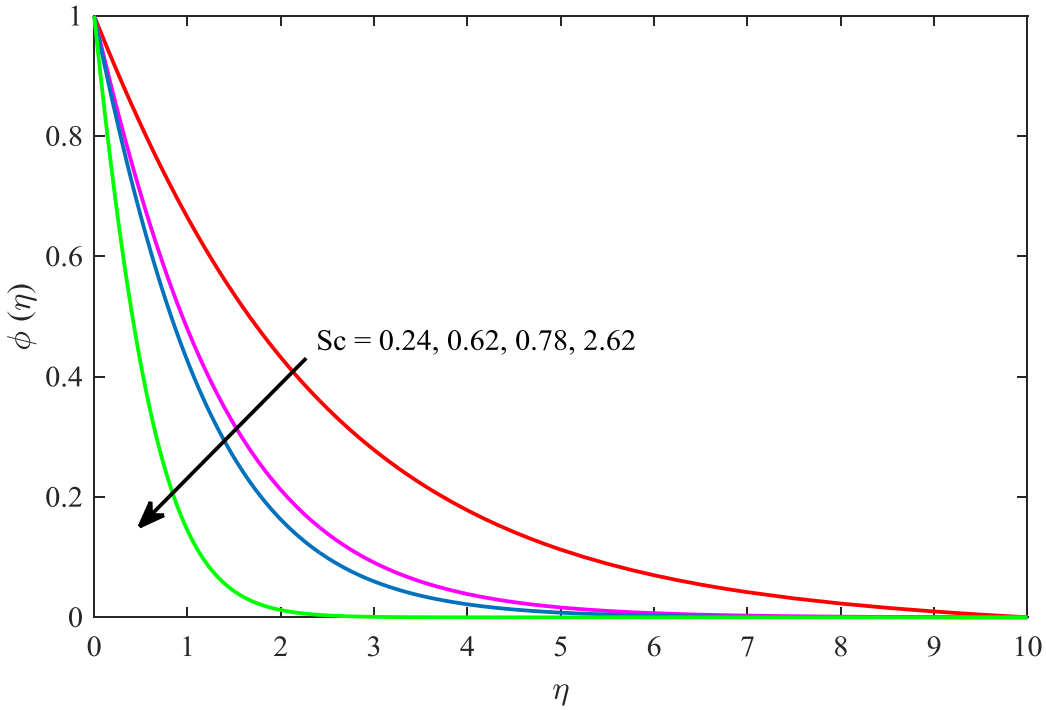

Fig. 8: Concentration distribution $\phi(\eta)$ for diverse morals of Sc .

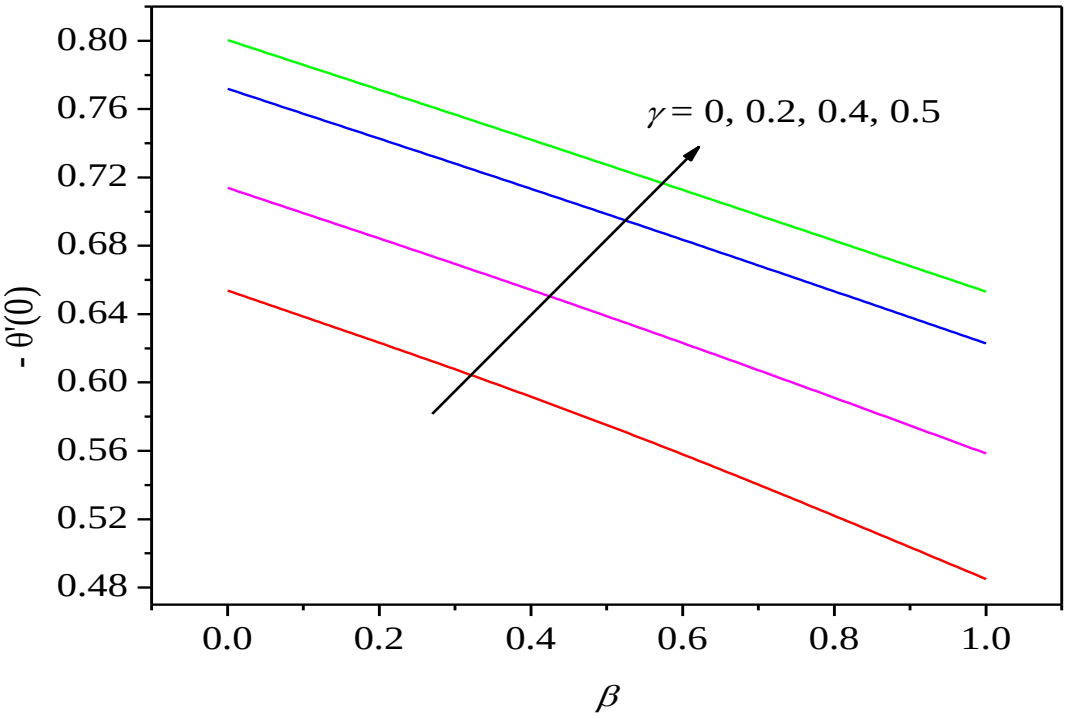

Fig. 9: Local Nusselt number $-\theta'(0)$ for diverse morals of β and γ .

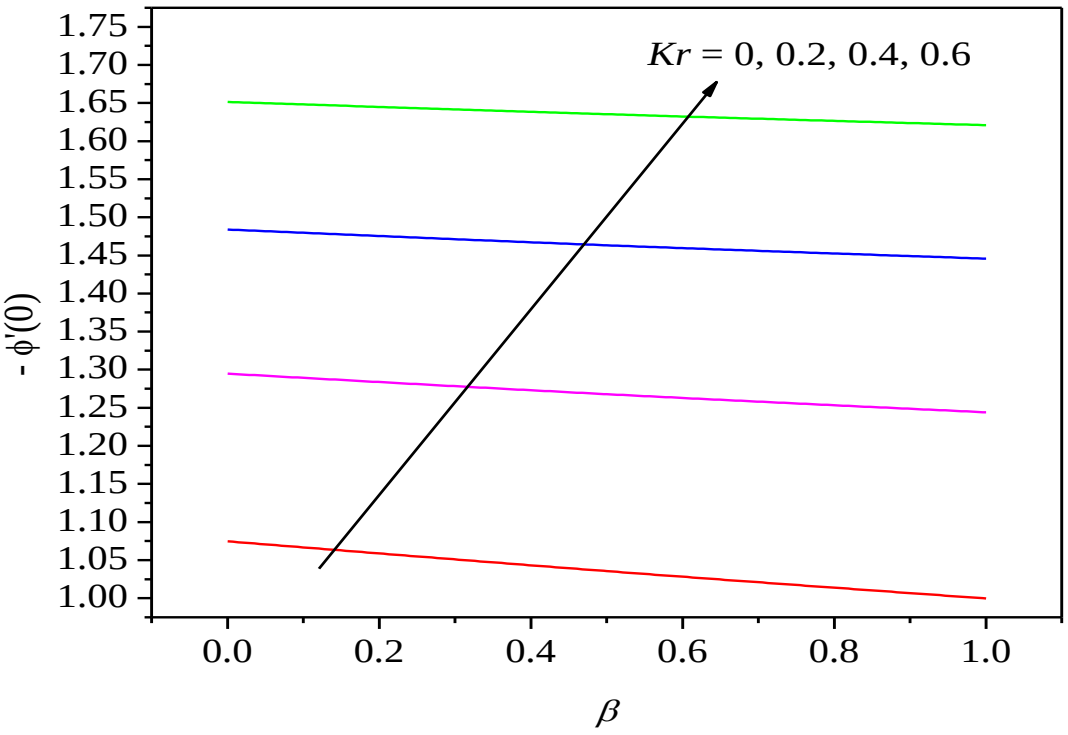

Fig. 10: Local Sherwood number $-\phi'(0)$ for diverse morals of β and Kr .

Table 1 Judgment of skin friction coefficient $-f''(0)$ with the on hand domino effects in prose for diverse morals of β when $Pr = 1, \gamma = 0.1$, $Q = Sc = Kr = 0$.

β	$-f''(0)$		
	Siri et al. [23] RK Gill	Siri et al.[23] HWQM	Present results
0.1	1.02654	1.02653	1.026189
0.15	1.03940	1.03939	1.039100
0.2	1.05215	1.05214	1.051893

Table 2 Judgment of local Nusselt number $-\theta'(0)$ with the on hand domino effects in literature for diverse morals of γ and β when $Pr = 1$, $Q = Sc = Kr = 0$.

γ	$-\theta'(0)$								
	$\beta = 0.1$			$\beta = 0.15$			$\beta = 0.2$		
	Siri et al. [23] RK Gill	Siri et al.[23] HWQM	Present results	Siri et al. [23] RK Gill	Siri et al.[23] HWQM	Present results	Siri et al. [23] RK Gill	Siri et al.[23] HWQM	Present results
0.1	0.58379	0.58379	0.582336	0.57983	0.57983	0.578133	0.57593	0.57593	0.573993
0.4	0.61014	0.61014	0.610209	0.60553	0.60554	0.605492	0.60101	0.60101	0.600847
0.5	0.61998	0.61998	0.620220	0.61516	0.61516	0.615321	0.61042	0.61042	0.610497
0.6	0.63029	0.63029	0.630600	0.62526	0.62526	0.625516	0.62031	0.62031	0.620508
0.8	0.65215	0.65215	0.652486	0.64673	0.64673	0.647023	0.64138	0.64138	0.641639
1.0	0.67551	0.67551	0.675841	0.66972	0.66972	0.670007	0.66400	0.66400	0.664250

Table 3 Judgment of local Nusselt number $-\theta'(0)$ with the on hand domino effects in literature for diverse morals of *Pr* in the case of Newtonian fluid ($\beta = \gamma = Q = Sc = Kr = 0$).

Pr	$-\theta'(0)$						
	Wang [24]	Gorla and Sidawi [25]	Khan and Pop[26]	Malik et al. [27]	Siri et al.[23] HWQM	Siri et al. [23] RK Gill	Present results
0.7	0.4539	0.5349	0.4539	0.45392	0.453930	0.453917	0.454447
2	0.9114	0.9114	0.9113	0.91135	0.911345	0.911358	0.911353
7	1.8954	1.8905	1.8954	1.89543	1.895489	1.895403	1.895400
20	3.3539	3.3539	3.3539	3.35395	3.353905	3.353904	3.353902

REFERENCES

[1]. Fourier, J.B.J.: Théorie Analytic. De La Chaleur, Paris (1822)
[2]. Cattaneo, C.: Sulla conduzione del calore. Atti Semin. Mat. Fis. Univ. Modena Reggio Emilia 3, 83–101 (1948)
[3]. Christov, C.I.: On frame indifferent formulation of the Maxwell–Cattaneo model of finite speed heat conduction. Mech. Res. Commun. 36(4), 481–486 (2009)
[4]. Straughan, B.: Thermal convection with the Cattaneo–Christov model. Int. J. Heat Mass Transf. 53(1–3), 95–98 (2010)
[5]. Ciarletta, M., Straughan, B.: Uniqueness and structural stability for the Cattaneo–Christov equations. Mech. Res. Commun. 37(5), 445–447 (2010)
[6]. Tibullo, V., Zampoli, V.: A uniqueness result for the Cattaneo–Christov heat conduction model applied to incompressible fluids. Mech. Res. Commun. 38(1), 77–79 (2011)
[7]. Han, S., Zheng, L., Li, C., Zhang, X.: Coupled flow and heat transfer in viscoelastic fluid with Cattaneo–Christov heat flux model. Appl. Math. Lett. 38, 87–93 (2014)
[8]. Mustafa, M.: Cattaneo–Christov heat flux model for rotating flow and heat transfer of upper-convected Maxwell fluid. AIP Adv. (2015) https://doi.org/10.1063/1.4917306
[9]. Khan, J.A., Mustafa, M., Hayat, T., Alsaedi, A.: Numerical study of Cattaneo–Christov heat flux model for viscoelastic flow due to an exponentially stretching sheet. PLoS ONE (2015) https://doi.org/10.1371/journal.pone.0137363
[10]. Hayat, T., Farooq, M., Alsaedi, A., Al-Solamy, F.: Impact of Cattaneo–Christov heat flux in the flow over a stretching sheet with variable thickness. AIP Adv. (2015) https://doi.org/10.1063/1.4929523
[11]. Gangadhar, K., K.V. Ramana, O.D. Makinde, B.R. Kumar, MHD Flow of a Carreau Fluid Past a Stretching Cylinder with Cattaneo-Christov Heat Flux Using Spectral Relaxation Method, Defect and Diffusion Forum, Vol. 387, pp 91-105
[12]. Gangadhar K, Venkata Ramana, Dasaradha Ramaiah and B. Rushi Kumar, Slip Flow of a Nanofluid Over a Stretching Cylinder with Cattaneo-Christov Flux Model: Using SRM, International Journal of Engineering & Technology, 7 (4.10) (2018) 225-232
[13]. Imran Khan, M., Hayat, T., Khan, M. I. & Alsaedi, A. A modified homogeneous-heterogeneous reaction for MHD stagnation flow with viscous dissipation and Joule heating. Int. J Heat Mass Tran. 113, 310–317 (2017).
[14]. Hayat, T., Sajjad, R., Ellahi, R., Alsaedi, A. & Muhammad, T. Homogeneous-heterogeneous reactions in MHD flow of micropolar fluid by a curved stretching surface. J. Mol Liq. 240, 209–220 (2017).
[15]. Lu, D. et al. On three-dimensional MHD Oldroyd-B fluid flow with nonlinear thermal radiation and homogeneous–heterogeneous reaction. J. Brazilian Soc. Mech. Sci. Eng. 40(8), 387 (2018).
[16]. Abbas, Z. & Sheikh, M. Numerical study of homogeneous–heterogeneous reactions on stagnation point flow of ferrofluid with nonlinear slip condition. Chinese. J Chem Eng. 25(1), 11–17 (2017).
[17]. Nadeem, S., Ullah, N., Khan, A. U. & Akbar, T. Effect of homogeneous-heterogeneous reactions on ferrofluid in the presence of magnetic dipole along a stretching cylinder. Results. Phys. 7, 3574–3582 (2017).

[18]. Raju, C. S. K., Sandeep, N., and Prakash, J., Dual solutions for heat and mass transfer in MHD Jeffrey fluid in the presence of homogeneous-heterogeneous reactions. Front. Heat Mass Transfer. 7(1), 14 (2016).
[19]. Imad Khan, Malik, M. Y., Hussain, A. & Salahuddin, T. Effect of homogenous-heterogeneous reactions on MHD Prandtl fluid flow over a stretching sheet. Results. Phys. 7, 4226–4231 (2017).
[20]. Gangadhar, K., Suresh Kumar, Ch., & Ranga Rao, T., A spectral relaxation approach for diffusion thermo effect on tangent hyperbolic fluid past a stretching surface in the presence of chemical reaction and convective boundary condition, Computational Thermal Sciences, vol.**10**, no.5, pp.389-403, 2018.
[21]. Qasim M (2013) Heat and mass transfer in a Jeffrey fluid over a stretching sheet with heat source/sink. Alex Eng J 52:571–575
[22]. Gangadhar, K., Kannan, T., DasaradhaRamaiah, K., and Sakthivel, G., (2018), Boundary layer flow of nanofluids to analyse the heat absorption/generation over a stretching sheet with variable suction/injection in the presence of viscous dissipation, International Journal of Ambient Energy, DOI: 10.1080/01430750.2018.1501738
[23]. Siri Z., Nor Artisham Che Ghani and Ruhaila Md. Kasmani, Heat transfer over a steady stretching surface in the presence of suction, Boundary Value Problems (2018) 2018:126, https://doi.org/10.1186/s13661-018-1019-6
[24]. Wang, C.Y.: Free convection on a vertical stretching surface. J. Appl. Math. Mech. 69(11), 418-420 (1989)
[25]. Gorla, R.S.R., Sidawi, I.: Free convection on a vertical stretching surface with suction and blowing. Appl. Sci. Res. 52(3), 247-257 (1994)
[26]. Khan, W.A., Pop, I.: Boundary-layer flow of a nanofluid past a stretching sheet. Int. J. Heat Mass Transf. 53(11-12), 2477-2483 (2010)
[27]. Malik, R., Khan, M., Shafiq, A., Mushtaq, M., Hussain, M.: An analysis of Cattaneo-Christov double-diffusion model for sisko fluid flow with velocity slip. Results Phys. 7, 1232-1237 (2017).

M. Sreedhar Babu, et. al. "Numerical solution for boundary layer flow of a Maxwell fluid over a stretched surface with Cattaneo-Christov heat flux in the presence of heat generation and chemical reaction." *International Journal of Mathematics and Statistics Invention (IJMSI)*, vol. 09(03), 2021, pp. 20-31.